NEW SCALE SENSITIVITY/UNCERTAINTY CAPABILITIES APPLIED TO BIAS ESTIMATION AND TO DESIGN OF MIRTE REFERENCE EXPERIMENTS

Bradley T. Rearden
Oak Ridge National Laboratory, P.O. Box 2008, Bldg. 5700, Oak Ridge, TN 37831-6170, USA
reardenb@ornl.gov

Isabelle Duhamel, Eric Létang
Institut de Radioprotection et de Sûreté Nucléaire, BP 17 - 92262 Fontenay aux Roses Cedex, France
isabelle.duhamel@irsn.fr

New TSUNAMI tools of SCALE 6, TSURFER and TSAR, are demonstrated to examine the bias effects of small-worth test materials, relative to reference experiments. TSURFER is a data adjustment bias and bias uncertainty assessment tool, and TSAR computes the sensitivity of the change in reactivity between two systems to the cross-section data common to their calculation. With TSURFER, it is possible to examine biases and bias uncertainties in fine detail. For replacement experiments, the application of TSAR to TSUNAMI-3D sensitivity data for pairs of experiments allows the isolation of sources of bias that could otherwise be obscured by materials with more worth in an individual experiment. The application of TSUNAMI techniques in the design of nine reference experiments for the MIRTE program will allow application of these advanced techniques to data acquired in the experimental series.

I. INTRODUCTION

The validation of all materials in a complex criticality safety application likely requires consolidating information from many different critical experiments. For certain materials, such as structural materials or fission products, only a limited number of critical experiments are available, and the fuel and moderator compositions of the experiments may differ significantly from those of the application. In these cases, it is desirable to extract the computational bias of a specific material from an integral k_{eff} measurement and use that information to quantify the bias due to the use of the same material in the application system.

Traditional parametric and nonparametric methods are likely to prove poorly suited for such a consolidation of specific data components from a diverse set of experiments. An alternative choice for consolidating specific data from numerous sources is a data adjustment tool, like the ORNL tool TSURFER (**T**ool for **S**ensitivity/**U**ncertainty analysis of **R**esponse **F**unctionals using **E**xperimental **R**esults) from SCALE 6.[1] However, even with TSURFER, it may be difficult to examine a single experiment and differentiate bias due to a test material from bias due to other materials such as fuel and moderator.

An alternative method is to perform two experiments on the same critical assembly, one with and one without the test material, and examine differences in the biases due to the introduction of the test material. Techniques to extract a computational bias from pairs of replacement experiments and project that bias, with an associated bias uncertainty, to an application system are described herein.

II. TSUNAMI SENSITIVITY AND UNCERTAINTY DATA

The k_{eff} sensitivity coefficients computed with SCALE/TSUNAMI have been documented and applied in numerous studies.[2,3] TSUNAMI also provides tools to quantify uncertainties in k_{eff} due to cross-section covariance

data and to assess overall similarity using the sensitivity and uncertainty (S/U) based integral index c_k. The c_k similarity index has been applied in trending analyses to compute biases and bias uncertainties.

In brief, the TSUNAMI-1D and TSUNAMI-3D sequences of SCALE 6 compute the sensitivity of k_{eff} to the group-wise cross-section data input to the calculation for systems that can be modeled with XSDRNPM, KENO V.a, or KENO-VI, as

$$S_{k,\sigma^i_{x,g}} = \frac{\Delta k/k}{\Delta\sigma^i_{x,g}/\sigma^i_{x,g}}, \tag{1}$$

where

k = k_{eff}

$\sigma^i_{x,g}$ = cross section for reaction x, of isotope i, energy group g.

Uncertainties in the cross-section data are represented in a multi-group cross-section-covariance data file distributed with SCALE 6. The uncertainty in the computed k_{eff} due to the uncertainties in the underlying cross-section data is quantified by propagating the covariance data to k_{eff} though the sensitivity coefficients.

The basis of the TSUNAMI validation techniques is that computational biases are primarily caused by errors in the cross-section data, which are quantified and bounded with a 1σ confidence by the cross-section-covariance data. For criticality code validation, k_{eff} sensitivity data are computed for the targeted application systems as well as relevant benchmark criticality experiments. The similarity of a benchmark experiment and an application system is quantified with a correlation coefficient, c_k, which quantifies the amount of shared uncertainty between the systems. Since the uncertainty is directly related to potential computational bias, c_k quantifies the similarity of the two systems in terms of common sources of bias. Where many benchmarks similar to the application are available to quantify all potential sources of bias, linear regression and extrapolation techniques can be applied to determine bias and bias uncertainty values for an application. However, where the benchmark experiments that thoroughly represent all aspects of an application are not available, it becomes difficult to justify the use of a combination of various experiments, each representing a portion of the application, to assess the overall bias and bias uncertainty of the application. In this case a data assimilation or data adjustment technique should be employed.

III. BIAS ASSESSMENT WITH TSURFER

A new capability for SCALE 6 allows the prediction of computational biases with the nuclear data adjustment tool TSURFER, which is based on a generalized linear least squares approach. TSURFER identifies a single set of adjustments to nuclear data that will result in the computational models all producing k_{eff} values close to their experimental k_{eff} value. Then the same data adjustments are used to predict an unbiased k_{eff} value for the application and an uncertainty on the adjusted k_{eff} value. The difference between the originally calculated k_{eff} value and the new post-adjustment k_{eff} value represents the bias in the original calculation, and the uncertainty in the adjusted value represents the uncertainty in this bias. If similar experiments are available to validate the use of a particular nuclide in the application, the uncertainty of the bias for this nuclide is reduced. In TSURFER, experiments that are dissimilar from the application can still provide useful information for bias assessment if at least one material demonstrates similar sensitivities to those of the application. If similar experiments are not available to validate a particular nuclide, a high uncertainty in the bias for the given nuclide will result. Thus, with a complete set of experiments to validate important components in the application, a precise bias with a small uncertainty can be predicted. Where the experimental coverage is lacking, a bias can be predicted with an appropriately large uncertainty. As users gain experience with TSURFER, it is expected to become a preferred tool for rigorous bias and bias uncertainty determination, particularly for applications for which nearly identical critical experiments are not available.

IV. REACTIVITY SENSITIVITY COEFFICIENTS

Even an advanced tool like TSURFER can only provide high-quality biases with low uncertainties where appropriate experimental data are available. In the case of a replacement measurement for a structural material or fission product, the worth of the test material must be much greater than the experimental uncertainties. In this case, it is advantageous to employ a means of emphasizing the test material though the use of two highly correlated experiments, one with the test material and one without. For example, two critical experiments could have the same fuel-rod array geometry, but different water heights to compensate for the reactivity of the test material, such as the fission products experiments performed by IRSN in the Valduc facility, which will be described in another paper in this conference.[4] Since both experiments are critical, the change in k_{eff} between the two systems (the reactivity difference) would be zero, within experimental uncertainties. However, if there were a computational bias due to the test material, the computed reactivity between the two experiments would not be zero, as the experiment with the test material would have a different computational bias than the experiment without the test material. This replacement technique magnifies the effect of the test material because all other materials are nearly the same, and sources of uncertainty between the two experiments are highly correlated. The primary difference between the two measurements is the test material itself.

To utilize the measured bias of the test material, TSUNAMI k_{eff} sensitivity data are generated for each pair of experiments, and the SCALE 6 tool TSAR (**T**ool **S**ensitivity **A**nalysis of **R**eactivities) is applied to determine the sensitivity of the reactivity between the two systems to the cross-section data. TSAR determines on a nuclide-reaction and energy-dependent basis the sensitivity of *changes* in computed k_{eff} between two systems to the cross-section data. Thus, if the primary difference between two critical measurements is the test material, TSAR determines, on an energy dependent basis, how sensitive the bias is to the test material. TSURFER then determines the sources of bias, using not only k_{eff} sensitivity data but also reactivity sensitivity data. For the test material, TSURFER applies its data adjustment procedure to obtain a consistency between the computed and measured reactivity changes for each pair of systems, determining the best-estimate cross-section adjustments for the test material. The best-estimate cross-section adjustments are those that lead to a consistency between the computed and measured values for the experiments, whether the experimental value is k_{eff} or reactivity. The measured bias due to the test material is then projected to a bias in the application by multiplying the cross-section adjustments that eliminate the bias in the experiments by the application's k_{eff} sensitivity coefficients for the same material. This product gives the relative bias in the application's computed k_{eff} value due to the test material.

V. AVAILABLE REACTIVITY EXPERIMENTS

The *International Handbook of Evaluated Criticality Safety Benchmark Experiments*[5] (IHECSBE) contains many criticality experiments that represent or can be evaluated as highly correlated replacement experiments. Two series of experiments examined here contain fission products ^{149}Sm and ^{103}Rh in evaluations LEU-COMP-THERM-050 and LEU-COMP-THERM-079, respectively. Selected configurations from each evaluation were modeled with SCALE/TSUNAMI-3D-K5 with calculations performed with the 238-group ENDF/B-VII.0 cross-section data library.

V.A LEU-COMP-THERM-050

The LEU-COMP-THERM-050 series of experiments consists of a water-moderated and reflected low-enriched UO_2 (4.738 wt % ^{235}U) fuel rod array surrounding a Zircaloy tank containing ^{149}Sm solution. For each configuration, the approach to critical was conducted with variable water height. The evaluation documents 11 benchmark experiments containing ^{149}Sm and two reference cores where the central Zircaloy tank is filled with water. Some information regarding the cases examined for this work is shown in TABLE I.

TABLE I. LEU-COMP-THERM-050 Cases

Case	Solution Characteristics			Geometry		k_{eff}	
	Type	Poison Conc. (g/L)	Acidity (N)	Driver Array	Critical Height (cm)	Measured	Calculated (SCALE 6.0 ENDF/B-VII.0)
1	H_2O		0.014	23x23-25	61.381	1.0004 ± 0.001	0.9975 ± 0.0002
8	Sm	0.1048	0.0149	23x25-25	62.663	1.0004 ± 0.001	0.9955 ± 0.0002
12	Sm	0.2148	0.0155	25x23-35	80.776	1.0004 ± 0.001	0.9973 ± 0.0002
13	Sm	0.2148	0.0155	25x23-43	87.577	1.0004 ± 0.001	0.9977 ± 0.0002
14	Sm	0.6262	0.0190	25x25-39	83.948	1.0004 ± 0.001	0.9973 ± 0.0002
15	Sm	0.6262	0.0190	25x25-43	88.935	1.0004 ± 0.001	0.9978 ± 0.0002
16	Sm	0.6262	0.0190	25x25-45	84.553	1.0004 ± 0.001	0.9989 ± 0.0002
17	Sm	0.6262	0.0190	25x25-49	86.302	1.0004 ± 0.001	0.9987 ± 0.0002
18	Sm	0.6262	0.0190	25x25-53	88.415	1.0004 ± 0.001	0.9986 ± 0.0002

V.B LEU-COMP-THERM-079

The LEU-COMP-THERM-079 series of experiments consists of a water-moderated and reflected low-enriched UO_2 (4.31 wt % ^{235}U) fuel rod array with thin foils of ^{103}Rh inserted between the fuel pellets of some fuel rods. For each configuration, the approach to critical was conducted adding fuel rods. The evaluation documents ten benchmark experiments at two different pitches where three benchmarks at each pitch contain ^{103}Rh foils. Some information regarding the benchmarks is provided in TABLE II.

TABLE II. LEU-COMP-THERM-079 Cases

Case	Geometry					k_{eff}	
	Fuel Element Pitch (cm)	Number of Driver Elements	Number of Experiment Elements	Number of ^{103}Rh Foils	Nominal Thickness of ^{103}Rh Foils (micron)	Measured	Calculated (SCALE 6.0 ENDF/B-VII.0)
1	2.0	257	0	-	-	0.9999 ± 0.0016	0.9980 ± 0.0002
2	2.0	221	36	0	-	1.0002 ± 0.0016	0.9982 ± 0.0002
3	2.0	234	36	31	25	1.0005 ± 0.0016	0.9982 ± 0.0002
4	2.0	243	36	31	50	1.0006 ± 0.0016	0.9985 ± 0.0002
5	2.0	258	36	31	100	1.0004 ± 0.0016	0.9991 ± 0.0002
6	2.8	131	0	-	-	0.9994 ± 0.0008	0.9988 ± 0.0002
7	2.8	95	36	0	-	1.0002 ± 0.0008	0.9993 ± 0.0002
8	2.8	104	36	31	25	1.0008 ± 0.0008	1.0000 ± 0.0002
9	2.8	110	36	31	50	1.0003 ± 0.0008	0.9999 ± 0.0002
10	2.8	122	36	31	100	1.0008 ± 0.0008	1.0009 ± 0.0002

V.C Reactivity Differences

For reactivity critical experiments, it is desirable to quantify the bias that can be observed from the introduction of the test material. Reactivity is computed as

$$\rho = 1 - \lambda, \tag{2}$$

where $\lambda = 1/k_{eff}$.

In reactor physics, the difference in reactivity between two different states is often used to quantify the worth of changing some condition, such as moving a control rod. This same concept can be applied to pairs of critical experiments, which are similar except for the introduction of an additional material. Here two states are considered where state 1 is defined as the reference core without the test material, and state 2 is defined as a similar core with the test material. The reactivity difference between the two cores is defined as

$$\rho_{1\to 2}^{m} = \rho_2^m - \rho_1^m = \lambda_1^m - \lambda_2^m, \tag{3}$$

where the indices 1 and 2 indicate each state and m indicates a measured quantity.

The uncertainty in the measured reactivity difference is derived from the individual experimental uncertainties and their correlations as

$$\sigma_{\rho_{1\to 2}^{m}} = \left(\sigma_{k_1^m}^2 + \sigma_{k_2^m}^2 - 2c_{12}\sigma_{k_1^m}\sigma_{k_2^m}\right)^{1/2}, \tag{4}$$

where c_{12} is the correlation coefficient between the uncertainties of experiments 1 and 2 and the measured uncertainties in k_{eff}, $\sigma_{k_1^m}$ and $\sigma_{k_2^m}$ are obtained from the DICE database.

Similarly, the computed reactivity difference for the same systems can be quantified as

$$\rho_{1\to 2}^{c} = \rho_2^c - \rho_1^c = \lambda_1^c - \lambda_2^c, \tag{5}$$

where c indicates a computed quantity. The uncertainties in the computed quantities are computed from Monte Carlo statistics from uncorrelated k_{eff} calculations as

$$\sigma_{\rho_{1\to 2}^{c}} = \left(\sigma_{k_1^c}^2 + \sigma_{k_2^c}^2\right)^{1/2}. \tag{6}$$

An indication that there is a computation bias due to the test material is that $\rho_{1\to 2}^{c}$ differs from $\rho_{1\to 2}^{m}$. The uncertainties must also be considered in these calculations. Because the experiments are similar, the uncertainties due to the fuel, moderator, and other common components will be highly correlated. For the purposes of this study, correlation coefficients of 0.90 and 0.98 were assumed for LEU-COMP-THERM-050 configurations and LEU-COMP-THERM-079 configurations, respectively. The measured and computed reactivity differences between configurations of the critical experiments are shown in TABLE III in units of percent-milli-rho (pcm), or $\Delta k_{eff} \times 10^5$. Note that the values shown in TABLE III were computed with more precision than is shown in TABLE I and TABLE II. Because the measured and computed reactivity differences vary, it is possible that there is a bias due to test material in each series of experiments. However, with only this integral information, it is not possible to determine the source of the differences in the biases, which could be due to the test material or to some other source, such as differing geometries of the configurations. Obtaining the bias due to the test material and projecting it to an application requires advanced analysis techniques.

TABLE III. Reactivity Differences

Evaluation	States	Measured Reactivity Difference (pcm)	Computed Reactivity Difference (pcm)
LEU-COMP-THERM-050	1→8	0 ± 45	-196 ± 27
	1→12	0 ± 45	-11 ± 28
	1→13	0 ± 45	29 ± 28
	1→14	0 ± 45	-16 ± 28
	1→15	0 ± 45	31 ± 28
	1→16	0 ± 45	142 ± 28
	1→17	0 ± 45	125 ± 28
	1→18	0 ± 45	118 ± 28
LEU-COMP-THERM-079	2→3	30 ± 32	5 ± 28
	2→4	40 ± 32	32 ± 28
	2→5	20 ± 32	92 ± 28
	7→8	60 ± 16	68 ± 28
	7→9	10 ± 16	60 ± 28
	7→10	60 ± 16	164 ± 28

VI. SENSITIVITY ANALYSIS

To better understand the performance of each system, sensitivity data were generated for k_{eff} and reactivity responses. A representative sample of the sensitivity coefficients computed with TSUNAMI-3D-K5 and TSAR for the critical experiments is presented below.

VI.A k_{eff} Sensitvities

The TSUNAMI-3D-K5 k_{eff} sensitivities were computed using the parameter values shown in TABLE IV. To ensure quality calculations, all results were verified with direct perturbation calculations.

TABLE IV. TSUNAMI-3D-K5 Parameter Data Used in Analysis of Critical Experiments

Parameter	Description	Value
NPG	Number of particles per generation for the forward calculation	10,000
APG	Number of particles per generation for the adjoint calculation	30,000
GEN	Maximum number of generations for the forward calculation	2,600
AGN	Maximum number of generations for the adjoint calculation	2,800
NSK	Number of generations to skip before accumulating information for the forward calculation	100
ASK	Number of generations to skip before accumulating information for the adjoint case	300
SIG	Desired k_{eff} convergence for the forward calculation	0.0002
ASG	Desired k_{eff} convergence for the adjoint calculation	0.001
MSH	Size of spatial mesh for flux accumulation for LEU-COMP-THERM-050 and LEU-COMP-THERM-079, respectively	2.6 cm, 10 cm

The k_{eff} sensitivities for ^{235}U fission, ^{238}U n,gamma, and ^{149}Sm n,gamma from LEU-COMP-THERM-050 cases 001, 008, and 018 are shown in Fig. 1. Here it is can be observed that the ^{235}U fission and ^{238}U n,gamma sensitivities are quite similar between all cases. It can also be observed that the ^{149}Sm sensitivities are an order of

magnitude smaller than the other sensitivities. Note that case 001 does not contain samarium solution and thus does not have ^{149}Sm sensitivity. The k_{eff} sensitivities for ^{1}H elastic scattering for these same three experiments are shown in Fig. 2. Note that small differences can be observed between the three cases, especially between cases 001 and 018, where the high concentration of samarium necessitated an approximately 50% increase in the critical water height to compensate for the high reactivity of the samarium. These two cases will exhibit different neutron leakages, which affect the ^{1}H sensitivity profiles.

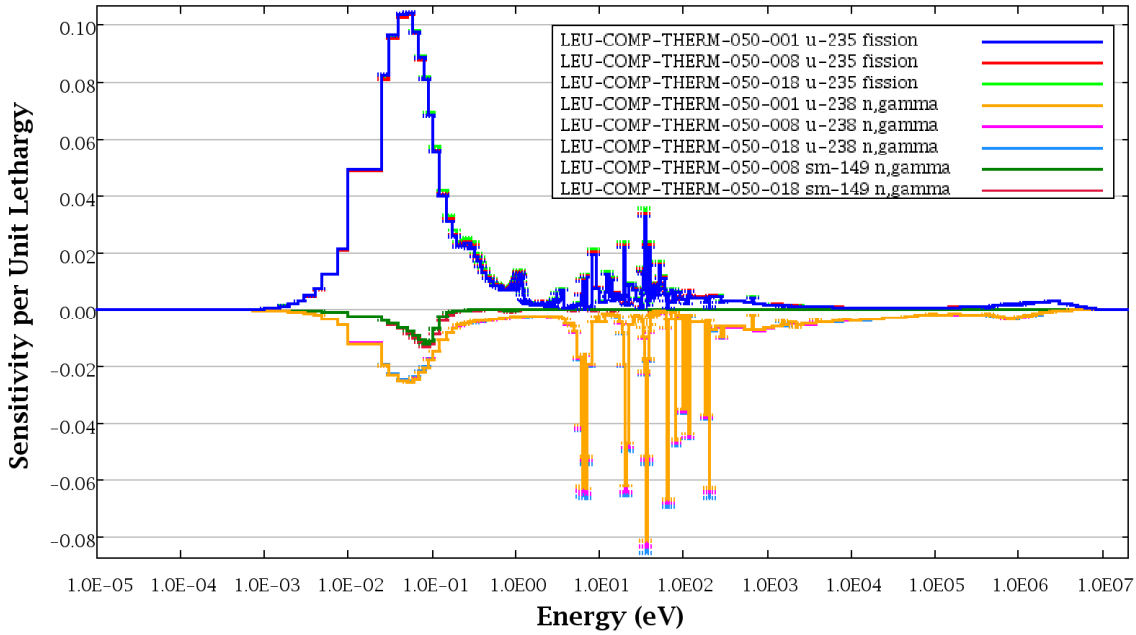

Fig. 1. k_{eff} sensitivities for ^{235}U fission, ^{238}U n,gamma and ^{149}Sm n,gamma from LEU-COMP-THERM-050 cases 001, 008 and 018.

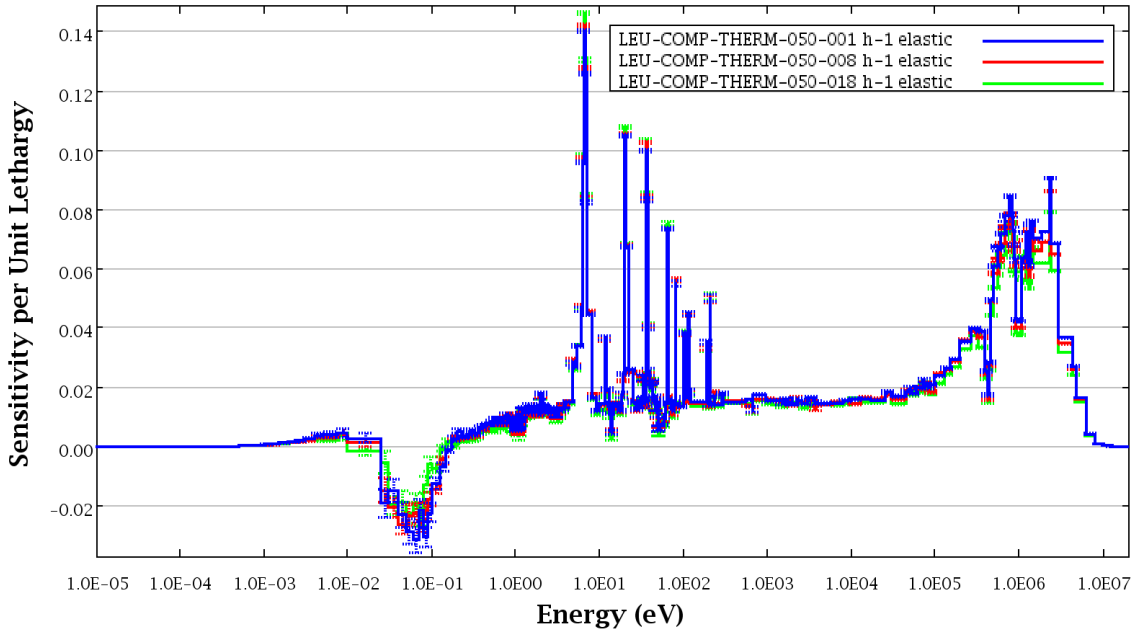

Fig. 2. k_{eff} sensitivities for ^{1}H elastic scattering from LEU-COMP-THERM-050 cases 001, 008 and 018.

The k_{eff} sensitivities for ^{235}U fission, ^{238}U n,gamma, and ^{103}Rh n,gamma from LEU-COMP-THERM-079 cases 002, 003, and 005 are shown in Fig. 3. As with LEU-COMP-THERM-050, the ^{235}U fission and ^{238}U n,gamma sensitivity profiles are similar for all three cases. Here, the rhodium sensitivities are much smaller than those of the other nuclides. The k_{eff} sensitivities for ^{1}H elastic scattering for these same three experiments are shown in Fig. 4. Here, the sensitivity profiles are mostly similar for all three cases, except that cases 003 and 005 exhibit a peak in the sensitivity just above 1 eV, corresponding to the ^{103}Rh resonance. In these experiments, ^{1}H elastic scattering in that energy range becomes more important because of the positive reactivity effect of escaping capture in ^{103}Rh.

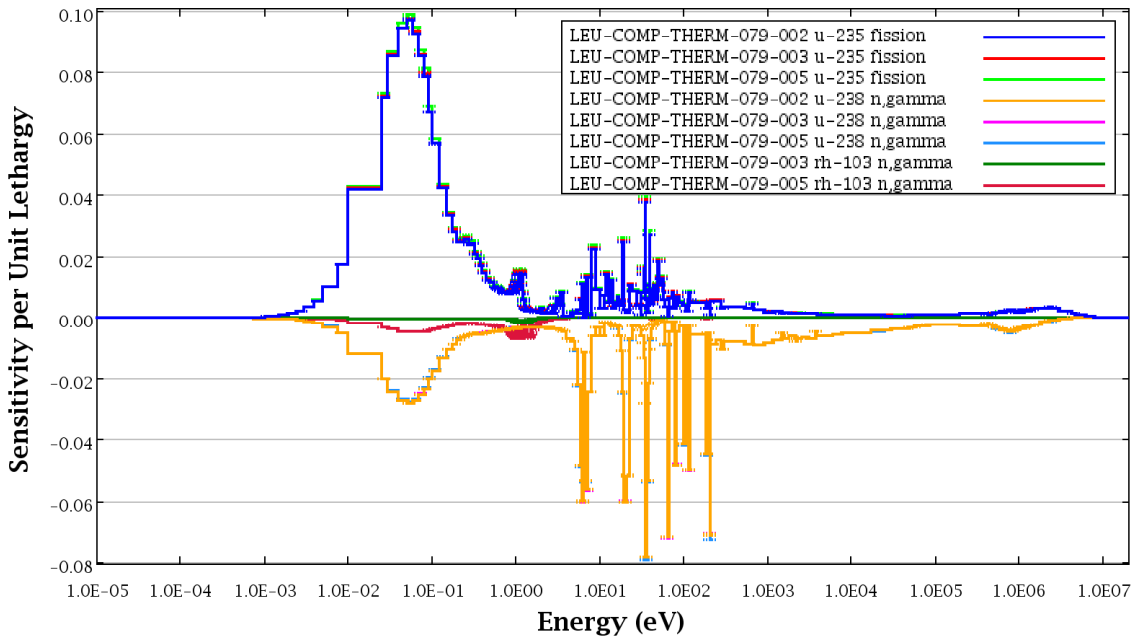

Fig. 3. k_{eff} sensitivities for ^{235}U fission, ^{238}U n,gamma and ^{103}Rh n,gamma from LEU-COMP-THERM-079 cases 002, 003 and 005.

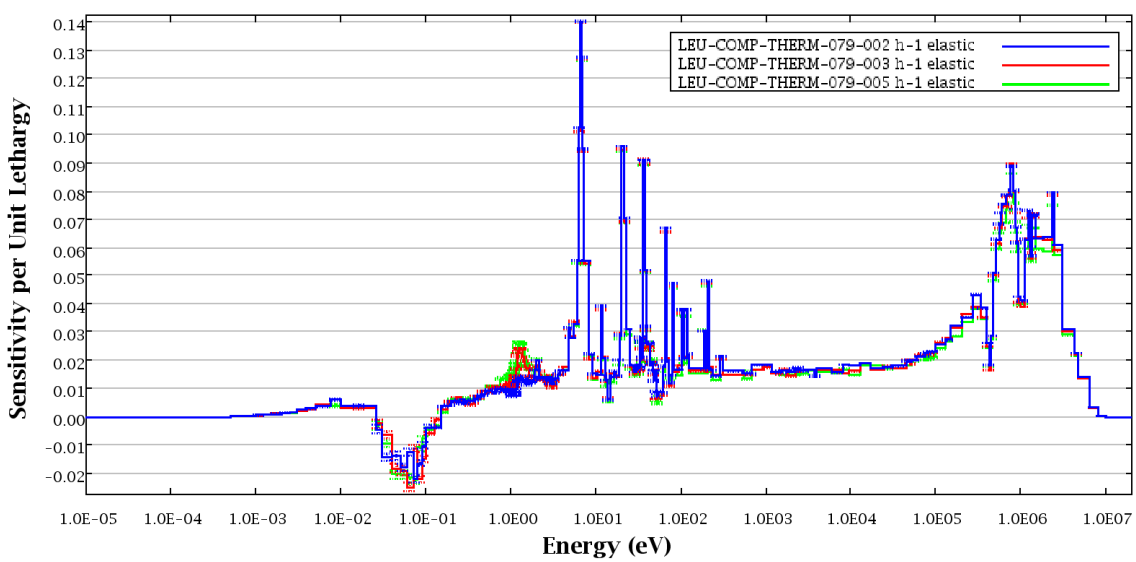

Fig. 4. k_{eff} sensitivities for ^{1}H elastic scattering from LEU-COMP-THERM-079 cases 002, 003 and 005.

VI.B Reactivity Sensitivities

The sensitivities of the computed reactivity difference between the pairs of experiments noted in TABLE III were computed with TSAR. The ρ sensitivities for ^{235}U fission, ^{238}U n,gamma, and ^{149}Sm n,gamma from LEU-COMP-THERM-050 case 001→008 are shown in Fig. 5. Because the ^{235}U fission and ^{238}U n,gamma k_{eff} profiles are quite similar between these two cases, ^{149}Sm n,gamma sensitivity is emphasized in the reactivity sensitivity coefficients. Because the reactivity change between the two cases is not very sensitive to ^{235}U fission or ^{238}U n,gamma, the -196 pcm reactivity difference shown in TABLE III is more likely due to ^{149}Sm n,gamma. However, as shown in Fig. 6, the ^{1}H elastic scattering differences between cases 001 and 008 do lead to reactivity sensitivities on the same order of magnitude as the ^{149}Sm sensitivities. Thus, it is possible that the reactivity difference is due to some combination of ^{1}H and ^{149}Sm.

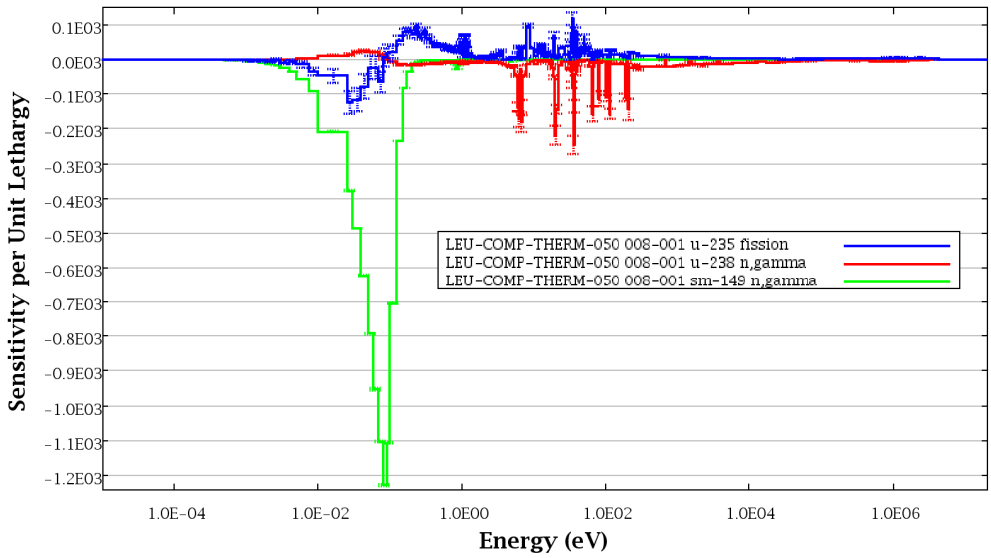

Fig. 5. Reactivity sensitivities for ^{235}U fission, ^{238}U n,gamma and ^{149}Sm n,gamma between LEU-COMP-THERM-050 cases 008 and 001.

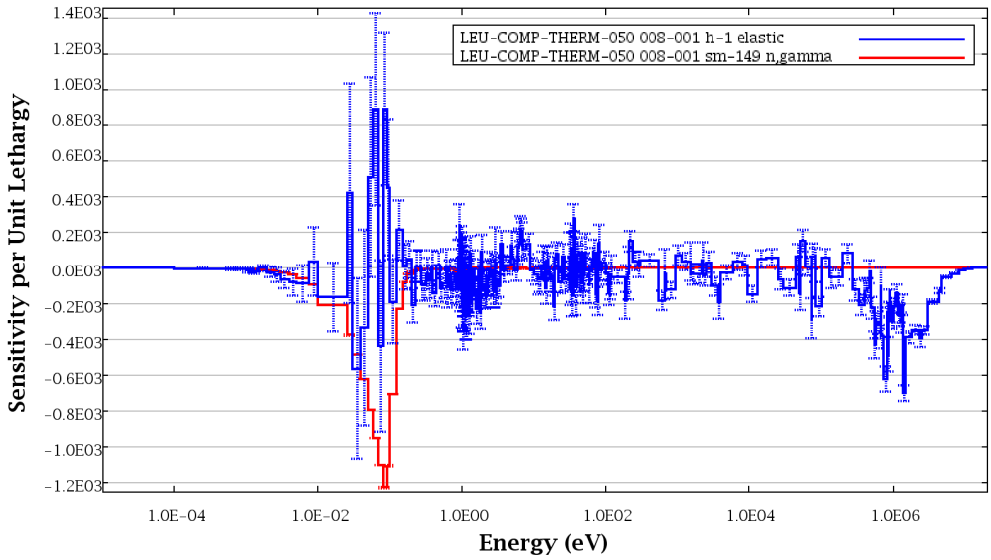

Fig. 6. Reactivity sensitivities for ^{1}H elastic scattering and ^{149}Sm n,gamma between LEU-COMP-THERM-050 cases 008 and 001.

The ρ sensitivities for ^{235}U fission, ^{238}U n,gamma, and ^{103}Rh n,gamma from LEU-COMP-THERM-079 case 002→005 are shown in Fig. 7. Because the ^{235}U fission and ^{238}U n,gamma k_{eff} profiles are similar between these two cases, the ^{103}Rh n,gamma sensitivity is emphasized in the reactivity sensitivity coefficients. However, the reactivity is somewhat sensitive to ^{235}U fission, indicating a shift in the ^{235}U fission sensitivities in the k_{eff} data. As shown in Fig. 8, the ^{1}H elastic scattering differences between cases 002 and 005 do lead to reactivity sensitivities that exceed the magnitude of the ^{103}Rh sensitivities. Thus, it is possible that the reactivity differences are due to some combination of effects from ^{1}H, ^{103}Rh, and ^{235}U.

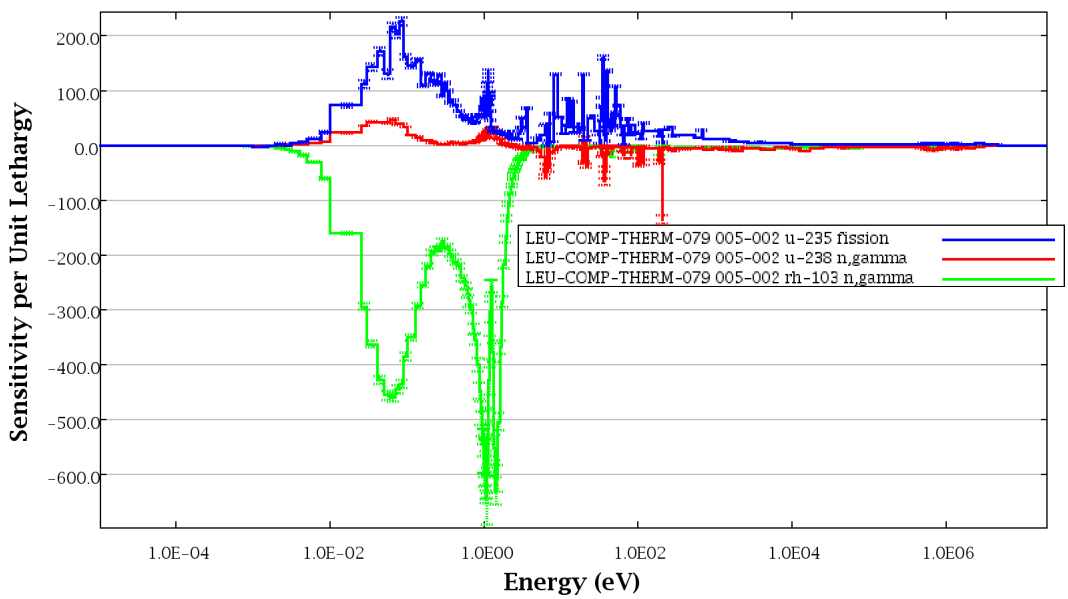

Fig. 7. Reactivity sensitivities for ^{235}U fission, ^{238}U n,gamma and ^{103}Rh n,gamma between LEU-COMP-THERM-079 cases 005 and 002.

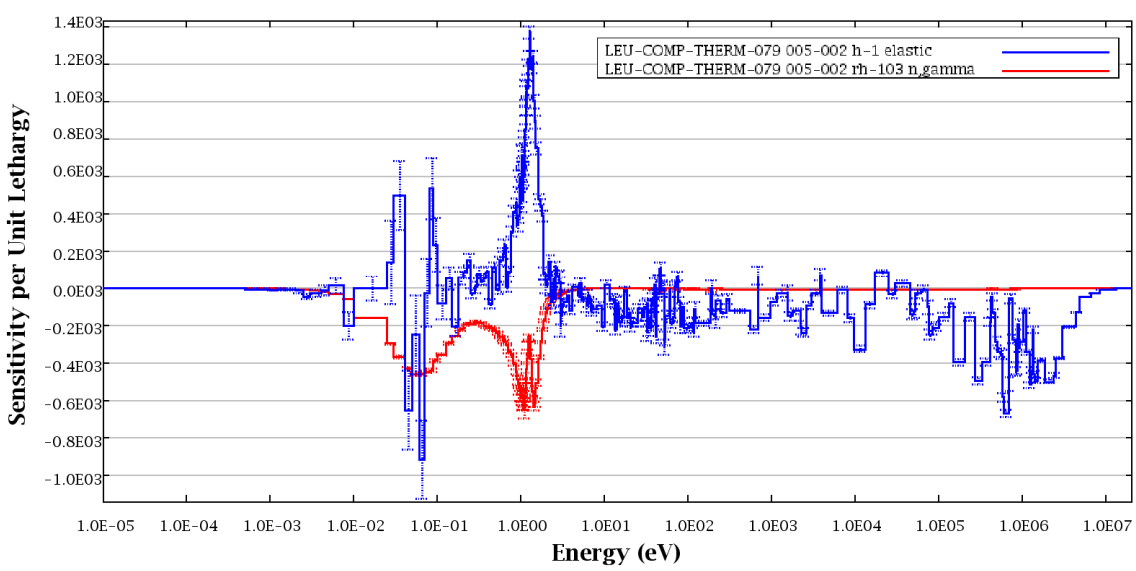

Fig. 8. Reactivity sensitivities for ^{1}H elastic scattering and ^{103}Rh n,gamma between LEU-COMP-THERM-079 cases 005 and 002.

VII. DATA ADJUSTMENT

The TSURFER module from SCALE 6.0 was applied to determine adjustments that lead to consistent calculated and measured results for many critical experiments.

VII.A Critical Experiments

A selection of critical experiments from the IHECSBE was included in this exercise. Experiments were included from evaluations HEU-MET-FAST-005 and -017; HEU-SOL-THERM-001 and -028; IEU-MET-FAST-002, 010, and 012; LEU-COMP-THERM-010, -017, -026, -042, and -049; MIX-COMP-FAST-001; MIX-COMP-MIXED-001; MIXED-COMP-THERM-002, -003, -004, -005, -006, -007, and -008; MIX-SOL-THERM-001, -002, -004, -005; and PU-SOL-THERM-005. As correlations in experimental uncertainties, required for TSURFER analysis, are currently not available in the IHECSBE, a correlation of 0.9 was assumed for experiments within a given evaluation. Furthermore, a correlation coefficient of 0.95 was assumed for reactivity data computed with TSAR using the same reference experiment.

VII.B k_{eff} Adjustment

An initial adjustment was performed with 121 experiments to identify cross-section adjustments in nuclides other than the fission products that could impact the calculated results for LEU-COMP-THERM-050 and -079. Some cross-section adjustments determined by TSURFER for this initial data adjustment are shown in Fig. 9.

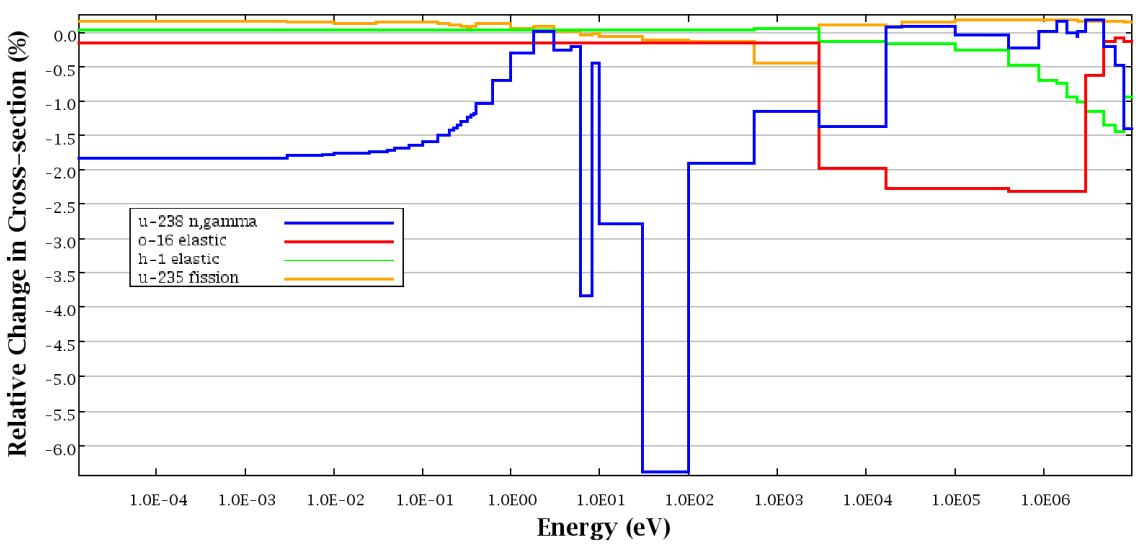

Fig. 9. Cross-section adjustments from k_{eff} adjustment procedure.

These cross-section adjustments were applied to determine adjusted k_{eff} values for the LEU-COMP-THERM-050 and -079 experiments. The original and adjusted k_{eff} values are shown in TABLE V, along with the original and adjusted uncertainty in k_{eff} due to cross-section-covariance data. The uncertainty due to cross-section-covariance data for each of these experiments was reduced from ~0.7% Δk/k to ~0.1% Δk/k, indicating good coverage by the 121 experiments active in the adjustment procedure for processes important to the fission products experiments. The initial adjustment should remove most sources of bias, except for biases caused by the fission products. The reactivity differences in the adjusted k_{eff} values are shown in TABLE VI.

TABLE V. Original and Adjusted k_{eff} and Uncertainty due to Cross-Section-Covariance Data

Evaluation	Case	Original Calculated k_{eff}	Original Uncertainty Due to Cross Sections (%Δk/k)	Adjusted k_{eff}	Adjusted Uncertainty Due to Cross Sections (%Δk/k)
LEU-COMP-THERM-050	1	0.9975	0.6672	1.0004	0.0994
	8	0.9955	0.6488	0.9984	0.1005
	12	0.9973	0.6281	1.0001	0.0999
	13	0.9977	0.6254	1.0005	0.0997
	14	0.9973	0.6167	1.0000	0.0987
	15	0.9978	0.6165	1.0005	0.0988
	16	0.9989	0.6194	1.0017	0.0990
	17	0.9987	0.6170	1.0015	0.0987
	18	0.9986	0.6147	1.0014	0.0983
LEU-COMP-THERM-079	1	0.9980	0.6986	1.0008	0.1092
	2	0.9982	0.6944	1.0010	0.1086
	3	0.9982	0.6856	1.0010	0.1079
	4	0.9985	0.6788	1.0012	0.1082
	5	0.9991	0.6678	1.0018	0.1099
	6	0.9988	0.6533	1.0013	0.0880
	7	0.9993	0.6526	1.0018	0.0877
	8	1.0000	0.6415	1.0025	0.0872
	9	0.9999	0.6331	1.0024	0.0885
	10	1.0009	0.6181	1.0033	0.0943

TABLE VI. Reactivity Differences After k_{eff} Adjustments

Evaluation	States	Adjusted Reactivity Difference (pcm)
LEU-COMP-THERM-050	1→8	-200
	1→12	-30
	1→13	10
	1→14	-40
	1→15	10
	1→16	130
	1→17	110
	1→18	100
LEU-COMP-THERM-079	2→3	0
	2→4	20
	2→5	80
	7→8	70
	7→9	60
	7→10	149

VII.C Adjustment Including Reactivity Sensitivity Data

A subsequent data adjustment was performed including the reactivity sensitivity data from TSAR in the active adjustment. Because the nuclides other than the fission products were constrained by the 121 other active experiments in the adjustment, negligible additional changes in those cross sections were introduced by adding the reactivity data into the adjustment. However, changes were realized for the fission product nuclides, as shown in Fig. 10. Note that the broad uniform changes in the cross sections across the thermal- and intermediate-energy regions are due to correlations in the SCALE cross-section-covariance data for ^{103}Rh and ^{149}Sm n,gamma reactions.

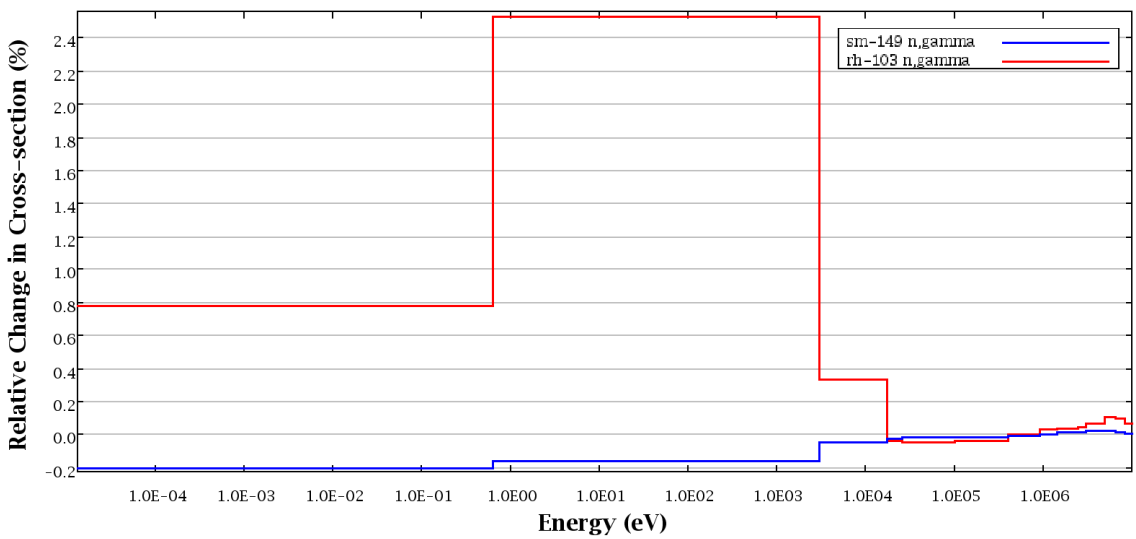

Fig. 10. Cross-section adjustments from k_{eff} and ρ adjustment procedure.

VIII. PROJECTION OF BIAS TO APPLICATION SYSTEM

The application system selected for bias determination is the GBC-32 burnup credit shipping cask model.[6,7] The GBC-32 cask model with the top half and front right quarter removed is shown in Fig. 11. The cask has 8 in. thick steel sides, top and bottom. The basket of the cask is formed from square stainless steel tubes with a Boral plate between each pair of assemblies and on the outsides of each peripheral assembly. The cask is modeled as flooded with full density water and loaded with 32 Westinghouse 17 × 17 optimized fuel assemblies (W17×17OFA) having initial enrichment of 4 wt % ^{235}U burned to 40 GWd/MTU and cooled for 5 years. The STARBUCS sequence of SCALE was used to generate 18 axial location-dependent burned fuel compositions. From the depletion calculations, fuel compositions for the following nuclides were retained for the criticality calculations: ^{234}U, ^{235}U, ^{236}U, ^{238}U, ^{237}Np, ^{238}Pu, ^{239}Pu, ^{240}Pu, ^{241}Pu, ^{242}Pu, ^{241}Am, ^{243}Am, ^{95}Mo, ^{99}Tc, ^{101}Ru, ^{103}Rh, ^{109}Ag, ^{133}Cs, ^{147}Sm, ^{149}Sm, ^{150}Sm, ^{151}Sm, ^{152}Sm, ^{143}Nd, ^{145}Nd, ^{151}Eu, ^{153}Eu, and ^{155}Gd. The fuel burnup calculations model the depletion of the ^{235}U and the in-growth of plutonium and selected fission product nuclides.

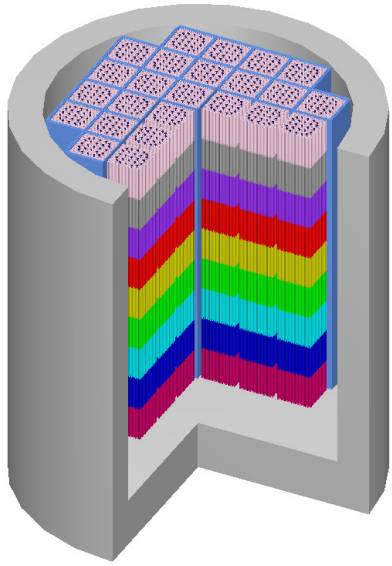

Fig. 11. Cut-away view of the GBC-32 cask model.

The SCALE 6.0 ENDF/B-VII.0 calculation of the GBC-32 cask models produces a k_{eff} of 0.9429 ± 0.0005 with an uncertainty due to cross-section covariance data of 0.52% Δk/k. Thus, the computational bias of this model is expected to be less than 0.52% Δk/k with a 1σ confidence. With the initial TSURFER calculation, all cross-section adjustments, including those shown in Fig. 9, are projected to a change in k_{eff} for the GBC-32 model through its sensitivity coefficients. Also, the adjusted cross-section covariance data are applied to determine an uncertainty in the bias. The initial adjustment results in a computational bias of -0.072% Δk/k with a bias uncertainty of 0.11% Δk/k. Note that the initial adjustment reduced the uncertainty from 0.52% Δk/k to 0.11% Δk/k, nearly an 80% reduction in uncertainty with the inclusion of the benchmark set. This initial bias uncertainty includes uncertainties due to ^{103}Rh n,gamma and ^{149}Sm n,gamma, which are 0.0213% Δk/k and 0.0216% Δk/k, respectively.

After the second adjustment, including the fission product experiment reactivity sensitivity data, the overall bias changed to -0.024% Δk/k with a bias uncertainty of 0.10% Δk/k. Because TSURFER determines bias from adjustments of the cross-section data, the contributions to the bias from individual nuclide-reaction pairs can be determined, as shown in TABLE VII for the top 26 contributors to the bias, including ^{103}Rh and ^{149}Sm. Additionally, when the energy-dependent cross-section adjustments are multiplied by the sensitivity of the application k_{eff} to the same cross-section data, the bias can be quantified on an energy-dependent nuclide-reaction specific basis, as shown in Fig. 12. From both TABLE VII and Fig. 12, it is evident that the small overall bias in the GBC-32 cask model is due to the summation of positive and negative biases from various sources. However, TSURFER provides a unique ability to reveal the individual contributors to the bias.

TABLE VII. Contributions to Bias by Individual Nuclear-Reaction Pairs

Nuclide	Reaction	Contribution to Bias (%Δk/k)
U-238	n,gamma	-0.360
Pu-239	nubar	0.192
U-235	nubar	0.073
Pu-239	n,gamma	-0.058
Pu-239	fission	0.040
O-16	elastic	0.041
H-1	elastic	0.019
U-235	chi	0.001
Fe-56	n,gamma	-0.027
U-235	n,gamma	0.025
Pu-239	chi	0.014
U-238	elastic	-0.005
Pu-240	n,gamma	-0.013
Rh-103	n,gamma	0.014
U-238	n,n'	-0.010
U-235	fission	0.000
Zr-92	n,gamma	0.008
U-238	nubar	0.007
B-10	n,alpha	0.006
Am-241	n,gamma	0.005
H-1	n,gamma	0.005
Zr-90	elastic	-0.005
Zr-91	n,gamma	0.004
Fe-56	elastic	0.000
Zr-90	n,gamma	0.003
Sm-149	n,gamma	-0.003

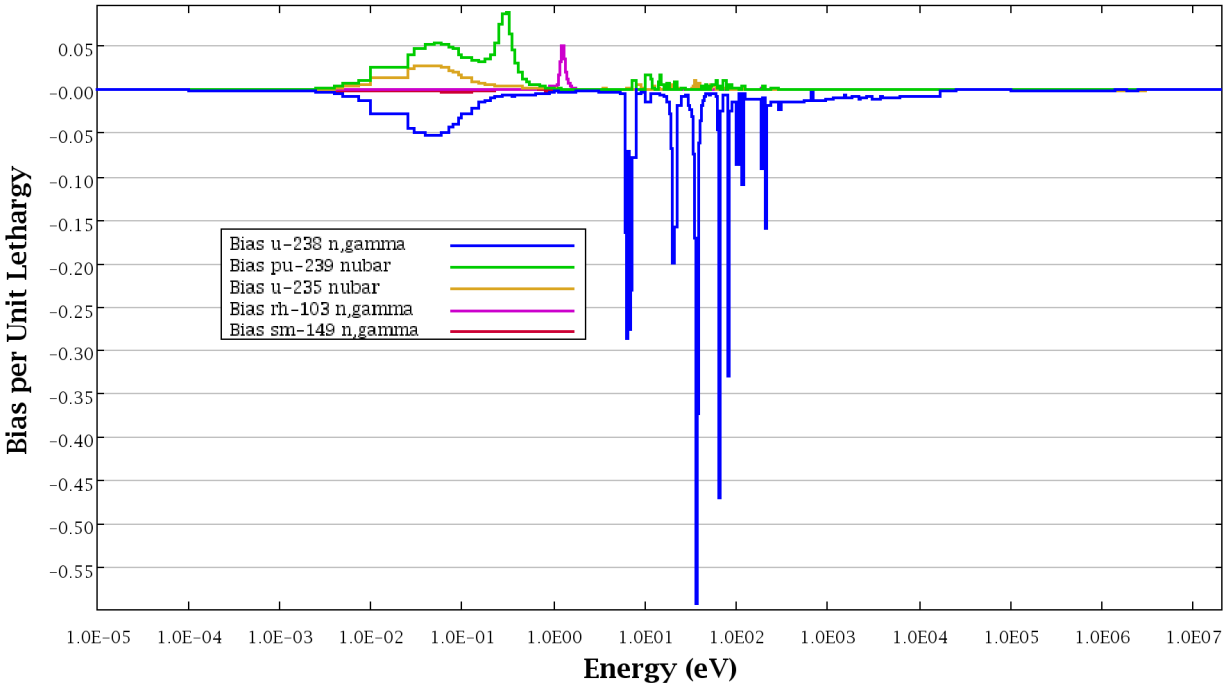

Fig. 12. Energy-dependent nuclide-reaction-specific bias in application.

Additionally, the uncertainty in the bias can be viewed according to its contributions from the adjusted cross-section covariance matrices, as shown in TABLE VIII. After the adjustment procedure, the remaining unvalidated components of the cross-section data are correlated because they were adjusted using the same set of experimental data. A number of anti-correlations appear in the data, which reduce the overall uncertainty in the bias. For example, ^{149}Sm and ^{103}Rh each have a positive uncertainty contribution from the n,gamma to n,gamma covariance matrix. However, this positive contribution to the bias uncertainty is partially offset by the cross-nuclide anti-correlated covariance with ^{235}U nubar introduced in the adjustment procedure.

TABLE VIII. Contribution to Bias Uncertainty by Covariance Matrix

Covariance Matrix			Contribution to Bias Uncertainty (%Δk/k)
^{239}Pu fission		^{239}Pu nubar	-0.172
^{239}Pu nubar		^{239}Pu nubar	0.163
^{239}Pu n,gamma		^{239}Pu nubar	-0.140
^{235}U nubar		^{235}U nubar	0.113
^{238}U n,gamma		^{238}U n,gamma	0.109
^{239}Pu fission		^{239}Pu fission	0.105
^{235}U n,gamma		^{235}U nubar	-0.092
^{239}Pu fission		^{239}Pu n,gamma	0.089
^{235}U fission		^{235}U nubar	-0.086
^{239}Pu n,gamma		^{239}Pu n,gamma	0.081
^{235}U nubar		^{238}U n,gamma	-0.080
^{1}H elastic		^{1}H elastic	0.070
^{235}U n,gamma		^{235}U n,gamma	0.070
^{238}U n,gamma		^{238}U nubar	-0.066
^{235}U fission		^{235}U fission	0.062
			…
^{149}Sm n,gamma		^{149}Sm n,gamma	0.018
^{149}Sm n,gamma		^{235}U nubar	-0.009
^{103}Rh n,gamma		^{103}Rh n,gamma	0.015
^{103}Rh n,gamma		^{235}U nubar	-0.010

IX. DESIGN OF REFERENCE CORES FOR MIRTE EXPERIMENTS

IX.A The MIRTE Experimental Program

A program focused on testing the reactivity effects of several structural/reflector materials that are important to criticality safety was initiated by the Institut de Radioprotection et de Sûreté Nucléaire (IRSN) in 2005.[8] In order to define the materials that would be tested, a priority list was established with French industrial partners, taking into account, on the one hand, the main structural materials encountered in criticality safety studies and, on the other hand, existing benchmarks available at that time[5] for the validation of criticality calculation codes and nuclear data. Finally, the experiments, which are being conducted in the Apparatus B facility of Valduc, will involve water-moderated low-enriched UO_2 (4.738 % enriched uranium) rods lattices with thermal energy spectra separated or reflected by plates made of different structural materials: iron, nickel, copper, aluminum, zircalloy, lead, glass (SiO_2), titanium and concrete with different water contents.

To better address the criticality validation needs, the critical configurations have been designed to ensure small experimental uncertainties (lower than 0.2 % on the k_{eff}) and optimum reactivity worth (greater than 4%) for each material.

Taking into account also technical feasibility constraints and fabrication costs, three different kinds of configurations were designed:

- two interacting arrays of UO_2 rods separated by a single test screen with thickness greater than 5 cm,
- four interacting arrays of UO_2 rods separated by thin cruciform plates with thickness less than 2 cm, and
- a single array of UO_2 rods reflected by structural materials.

The schematic views of these configurations are presented in Fig. 13.

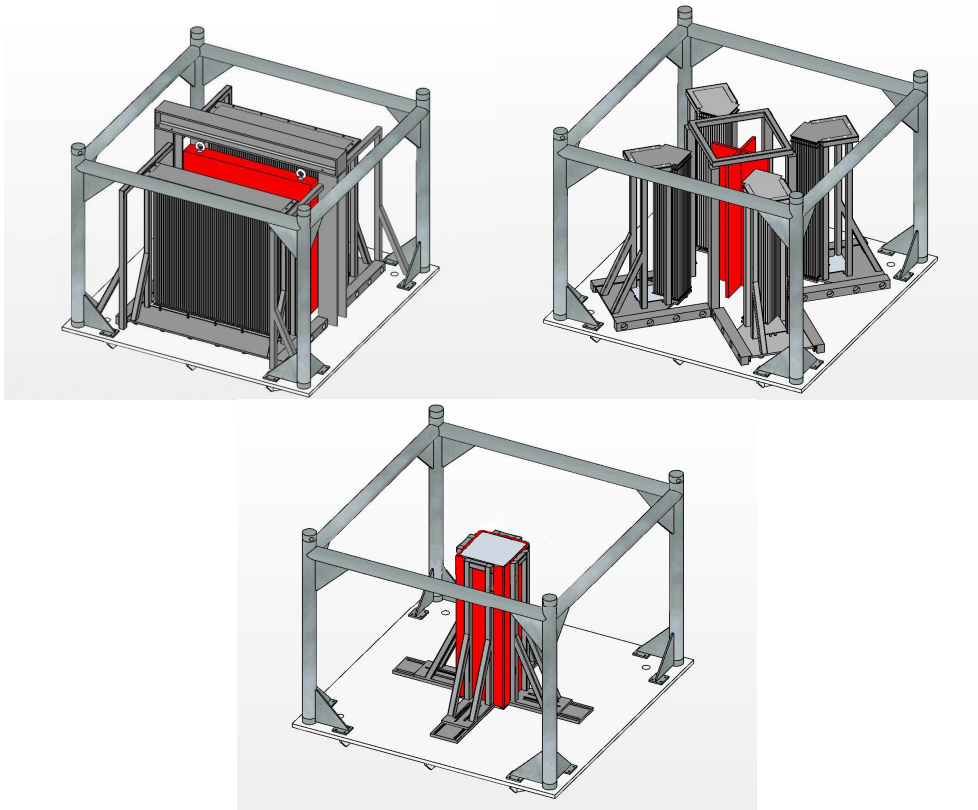

Fig. 13. Schematic view of the experimental devices.

In 2007, the project evolved into an international collaboration involving IRSN, the French energy group AREVA, the French National Radioactive Waste Management Agency ANDRA (Agence Nationale pour la gestion des Déchets Radioactifs), and the United States Department of Energy (DOE) and has officially been designated as MIRTE (Matériaux Interaction Réflexion Toutes Epaisseurs). About 40 critical configurations were planned in this framework.

IX.B Design of Reference Experiments

IRSN has extensive experience in peforming "reference experiments," also named replacement experiments, in order to evaluate an eventual bias due to a test element. This is the case, for example, for LEU-COMP-THERM-050 experiments[5] for ^{149}Sm validation and for the fission products program[4] for burnup credit validation. These reference experiments in each series emphasize the effect of the test element because the configurations are nearly the same and the primary difference between the two critical water height measurements is due to the test element itself.

For the MIRTE experimental program, some reference and reproducibility experiments were planned since the program inception, but efforts were mainly focused on the design of critical configurations involving the test material in 2005 to 2007. Thus, 19 configurations involving the various structural materials of interest were planned.

In 2008, the design of the reference experiments of the MIRTE program was optimized using the SCALE 5.1 sensitivity capabilities. The TSUNAMI-3D sequence of SCALE 5.1 was used to compute the sensitivity of k_{eff} to the group-wise cross-section data input to the calculation for MIRTE configurations. All calculations were performed using KENO-V.a code and 238-group ENDF/B-VI cross-section data. Fig. **14** shows examples of the computed configurations.

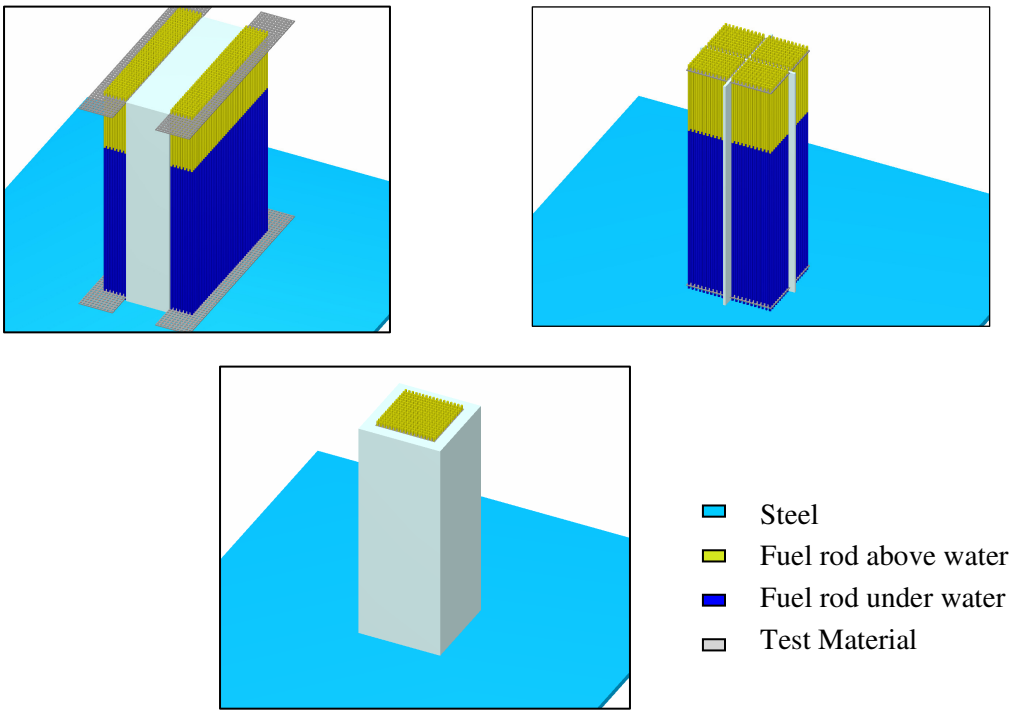

Fig. 14. SCALE 5.1 computed configurations.

As experiments performed in Apparatus B are critical experiments, the water height and/or the number of UO_2 rods in the arrays were varied to compensate for the reactivity of the test material. It was accepted to vary the water height to provide better coincidence for the sensitivity profiles, taking into account that, when keeping the array dimensions, the predicted critical water height can be very low, which can lead to significant experimental uncertainty.

The sensitivity profiles for each pair of experiments were compared using Javapeño plotting capabilities of SCALE 5.1. The aim of the study was to reach a similarity of the sensitivity profiles for the major actinides and moderator materials involved in every pair of the replacement experiments, as shown in Fig. 15 for an example experiment pair with and without titanium plates.

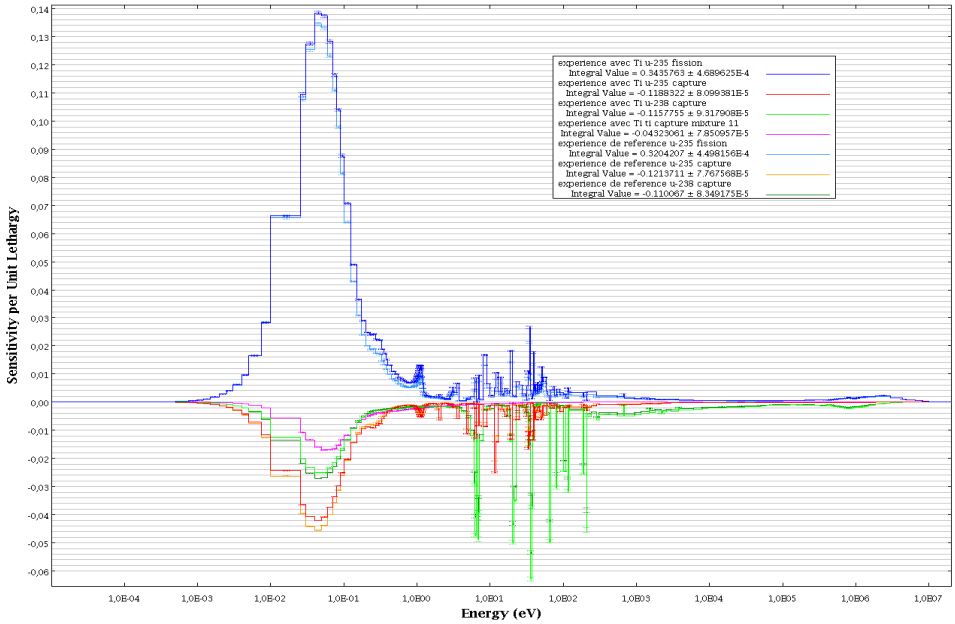

Fig. 15. Comparison of sensitivity profiles for uranium cross sections between experiments with and without test material—10 mm thick titanium cruciform plates.

As expected, the k_{eff} sensitivities for the test material are one order of magnitude lower than those of uranium cross sections.

Since both experiments are critical, the change in k_{eff} between the two systems (the reactivity difference) would be zero, within experimental uncertainties. Because TSAR was unavailable prior to SCALE 6, the plot operations of Javapeño were used to generate the k_{eff} sensitivity differences between the experiments with and without the test material, as shown in Fig. 16.

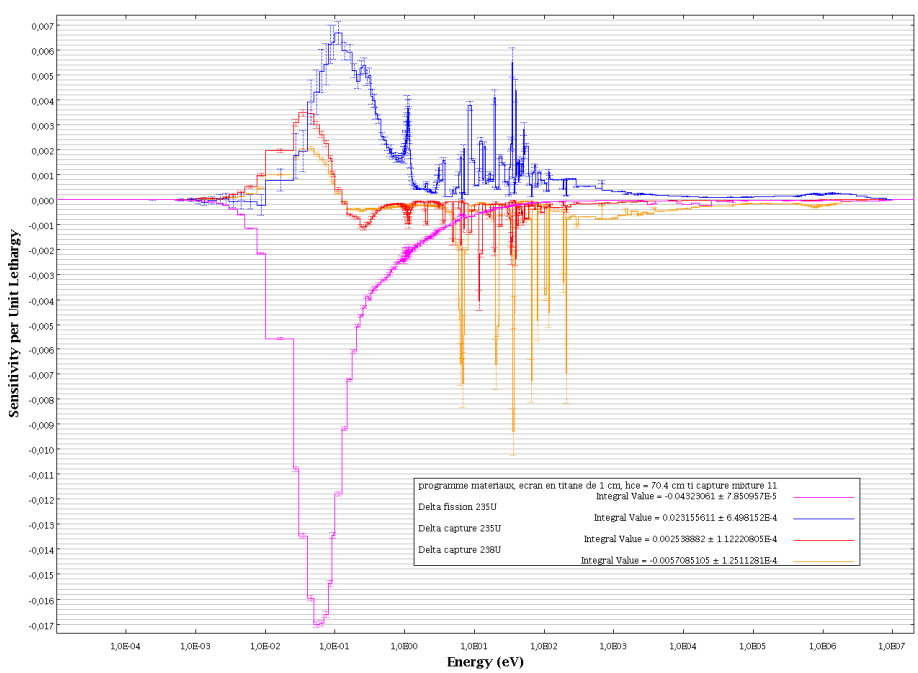

Fig. 16. Difference on sensitivity profiles for uranium cross sections between experiments with and without test material—10 mm thick titanium cruciform plates.

Based on the sensitivity studies, it was decided to perform nine reference experiments in the first phase of the MIRTE program.

Analyses of the Fission Product Experimental Program[4] and some other available experiments described in this paper have demonstrated the utility of performing replacement experiments to magnify the effect of the test material. As the MIRTE reference experiments were optimized (with the tools available in 2008) in order to have similar sensitivities profiles, they should prove useful in highlighting the effect of structural material. Thus, once the experiments are performed, the advanced tools of SCALE 6 can be applied to provide technical information for the evaluation of an eventual bias due to structural materials.

Moreover, in the scope of the second step of the MIRTE program, called MIRTE 2, the advanced sensitivity capabilities of the SCALE 6 code system (TSUNAMI, TSURFER, TSAR) will be used to design both kinds of experiments: experiments with new test structural materials and replacement configurations.

X. CONCLUSIONS

The new TSUNAMI tools of SCALE 6 have been demonstrated to examine the bias effects of small-worth test materials, relative to reference experiments. Applying the data adjustment bias assessment techniques of TSURFER, it is possible to examine biases and bias uncertainties in fine detail. With replacement experiments, the application of TSAR to TSUNAMI-3D sensitivity data for pairs of experiments allows the isolation of sources of bias differences that could otherwise be obscured by materials with more worth in an individual experiment. Nine reference experiments for the MIRTE program have been designed to allow application of these advanced techniques from data obtained in the experimental series.

REFERENCES

1. *SCALE: A Modular Code System for Performing Standardized Computer Analyses for Licensing Evaluation,* ORNL/TM-2005/39, Version 6, Vols. I–III, Oak Ridge National Laboratory, Oak Ridge, Tennessee, January 2009. Available from Radiation Safety Information Computational Center at Oak Ridge National Laboratory as CCC-750.
2. B. L. Broadhead, B. T. Rearden, C. M. Hopper, J. J. Wagschal, and C. V. Parks, "Sensitivity- and Uncertainty-Based Criticality Safety Validation Techniques," *Nucl. Sci. Eng*. **146**, 340–366 (2004).
3. D. E. Mueller, B. T. Rearden, and D. F. Hollenbach, *Application of the SCALE TSUNAMI Tools for the Validation of Criticality Safety Calculations Involving* ^{233}U, ORNL/TM-2008/196, Oak Ridge, Tenn., January 2009.
4. T. Ivanova et al., "Use of Fission Product Experiments for Burnup Credit Validation," submitted for publication, NCSD 2009.
5. *International Handbook of Evaluated Criticality Safety Benchmark Experiments*, Organization for Economic Cooperation and Development—Nuclear Energy Agency, NEA/NSC/DOC(95)03 (2008 Edition).
6. J. C. Wagner, *Computational Benchmark for Estimation of Reactivity Margin from Fission Products and Minor Actinides in PWR Burnup Credit*, NUREG/CR-6747 (ORNL/TM-2000/306), U.S. Nuclear Regulatory Commission, Oak Ridge National Laboratory, Oak Ridge, Tenn., October 2001.
7. D. E. Mueller and B. T. Rearden, "Sensitivity Coefficient Generation for a Burnup Credit Cask Model Using TSUNAMI-3D," presented at the 2005 NCSD Topical Meeting, Knoxville, TN, September 19–22, 2005.
8. I. Duhamel, "MIRTE: An Experimental Program Designed to Test the Reactivity Worth of Several Structural Materials," submitted for publication, NCSD 2009.